High CO2/N2/O2/CO separation in a chemically robust porous coordination polymer with low binding energy

Duan, J.; Higuchi, M.; Krishna, R.; Kiyonaga, T.; Tsutsumi, Y.; Sato, Y.; Kubota, Y.; Takata, M.; Kitagawa, S.

DOI
10.1039/c3sc52177j

Publication date
2014

Document Version
Final published version

Published in
Chemical Science

Chemical Science

EDGE ARTICLE

View Article Online
View Journal | View Issue

Cite this: *Chem. Sci.*, 2014, **5**, 660

High $CO_2/N_2/O_2/CO$ separation in a chemically robust porous coordination polymer with low binding energy†

Jingui Duan,[a] Masakazu Higuchi,[a] Rajamani Krishna,[b] Tomokazu Kiyonaga,[a] Yosuke Tsutsumi,[c] Yohei Sato,[d] Yoshiki Kubota,[de] Masaki Takata[e] and Susumu Kitagawa*[ac]

Received 3rd August 2013
Accepted 18th October 2013

DOI: 10.1039/c3sc52177j

www.rsc.org/chemicalscience

Porous coordination polymers (PCPs), constructed from organic linkers and metal ions, can provide special pore environments for selective CO_2 capture. Although many PCPs have been reported, a rational design for identifying PCPs that adsorb CO_2 molecules with a low binding energy, high separation ability and high chemical stability remains a great challenge. Here, we propose and validate, experimentally and computationally, a new PCP, [La(BTN)DMF]·guest (PCP-1⊃guest), that has a large aromatic organic surface and a low binding energy for high CO_2 separation from four-gas mixtures (CO_2–N_2–O_2–CO) at ambient temperature. In addition, it shows good water and chemical stability; in particular, it is stable from pH = 2 to 12 at 100 °C, which is unprecedented for carboxylate-based PCPs.

Introduction

CO_2 levels are now 45% higher than in 1990, a reference year for efforts to cut emissions.[1] Flue gases from coal-fired power and steel plants are the main contributors to this increase.[2] Usually, the flue gas contains mostly N_2, CO_2, and H_2O vapor as well as excess O_2 at *ca.* 1 bar. Some flue gases also contain small percentages of pollutants, such as CO, NO_x, and SO_x.[3] The development of efficient processes for capturing CO_2 is central to the reduction of the greenhouse gas emissions implicated in global warming.

Highly porous sorbent materials have been considered as plausible solutions for this problem, and this has driven a great deal of effort to design and construct these new adsorbent materials.[4] Porous coordination polymers (PCPs) and metal organic frameworks (MOFs) with high surface areas, periodic but tunable pore sizes and types and functionalizable pore walls are excellent rivals to other porous materials, such as zeolites and activated carbon, for gas storage and separation.[5]

To improve the capability of selective CO_2 capture by PCP materials, immobilizing strong recognition sites into the framework, such as dense open metal sites,[6] alkylamine functionalities,[7] and amine-based organic building blocks,[8] was considered a rational design, and indeed some PCPs show excellent separation behavior. However, the net energy cost of the regeneration process will be increased in frameworks with high binding energies (50–90 kJ mol^{-1}); furthermore, the modified frameworks are very sensitive to moisture which will greatly restrict their application in CO_2 capture, especially in industrial flue gas systems.[4]

Thus, for finding the optimal choice among PCPs, simply increasing the binding energy of CO_2 is not enough; the candidate should meet four prerequisites:[9] first, it should take up enough CO_2 in both static and dynamic environments at ambient temperature; second, the selectivity for CO_2 *vs.* other gases should be high; third, the degassed framework should maintain its structure in humid or aqueous environments; and finally and most importantly, the binding energy of the framework to CO_2 should permit a completely reversible adsorption and desorption process with a low energy penalty. Many PCPs can meet one or two of these prerequisites, but very few can satisfy all.[4–9]

A recent computational study found that, as a way to provide suitable physisorption energy (neither too high nor too low) of CO_2 in PCPs, the functionalization of organic linkers would be a good choice.[10] Currently, the organic linkers of most PCPs have backbones such as benzene rings, carbon–carbon triple bonds

[a]*Institute for Integrated Cell-Material Sciences (WPI-iCeMS), Kyoto University, Yoshida, Sakyo-ku, Kyoto 606-8501, Japan. E-mail: kitagawa@icems.kyoto-u.ac.jp*
[b]*Van 't Hoff Institute for Molecular Sciences, University of Amsterdam, Science Park 904, 1098 XH Amsterdam, The Netherlands*
[c]*Department of Synthetic Chemistry and Biological Chemistry, Graduate School of Engineering, Kyoto University, Katsura, Nishikyo-ku, Kyoto 615-8510, Japan*
[d]*Department of Physical Science, Graduate School of Science, Osaka Prefecture University, Sakai, Osaka 599-8531, Japan*
[e]*SPring-8 Center, RIKEN 1-1-1, Kouto, Sayo-cho, Sayo-gun, Hyogo 679-5148, Japan*

† Electronic supplementary information (ESI) available: Synthesis and characterization of PCP-1, PXRD, TGA, IR, sorption isotherms, IAST and breakthrough calculations, fitting parameters for PCP-1. CCDC 946972. For ESI and crystallographic data in CIF or other electronic format see DOI: 10.1039/c3sc52177j

and nitrogen–nitrogen double bonds, only a few of them involve larger aromatic rings such as naphthalene rings.[11]

Recently, we developed a strategy for using an organic wall to prepare [(La(BTB)H_2O)·solvent][12] structures that possess a high surface area, high CH_4 separation capability at 273 K, and also show high resistance to water, acid, and alkaline in particular; at pH = 14 and 100 °C. In that work, well-packed organic walls provided a hydrophobic channel environment that is appropriate for the pressure swing adsorption (PSA) process and provided water stability, even under harsh conditions. However, the CO_2 adsorption heat was too low (16–20 kJ mol^{-1}) to achieve good performance in CO_2 separation using PSA. Herein, in continuing our previous work, a linker (Scheme 1, H_3BTN) with larger aromatic rings was synthesized and employed in constructing the candidate PCP. Single crystal X-ray diffraction studies, pure gas adsorption experiments, ideal adsorbed solution theory predictions, packed bed absorber breakthrough simulations, and dynamic adsorption experiments revealed that the [La(BTN)DMF]·solvent (PCP-1⊃guest) could offer suitable uptake capacity as well as low binding energy to CO_2. Importantly, for the first time, good CO_2 separation abilities over N_2, O_2 and CO at 273 K were well characterized, even though the mixture includes four components. In addition, the material also shows good water and chemical stability; in particular, it is stable from pH = 2 to 12 at 100 °C, which is unprecedented for carboxylate-based PCPs. Thus, PCP-1 is a good potential candidate for CO_2 separation in the context of flue gas streams from coal-fired power and steel plants (CO_2–N_2, CO_2–O_2 and CO_2–CO), and other cases with four-gas mixtures (CO_2–N_2–O_2–CO) at ambient temperatures.

Experimental section

General procedures of the experiment and simulation can be found in the ESI.†

Synthesis of the organic building block

1,3,5-Tri(6-hydroxycarbonylnaphthalen-2-yl)benzene (H_3BTN) was synthesized according to the previous work.[11a]

Synthesis of [La(BTN)DMF]·solvent (PCP-1⊃guest)

$La(NO)_3·6H_2O$ (18 mg, 0.042 mmol), 1,3,5-tri(6-hydroxycarbonylnaphthalen-2-yl)benzene (H_3BTN, 6 mg, 0.01 mmol) and benzoic acid (75 mg, 0.614 mmol) were mixed with 1.25 mL DMF in a glass container, tightly capped with a Teflon vial and heated at 120 °C for 48 h. After cooling to room temperature, brown crystals were obtained. Yield: 62% (based on the ligand).

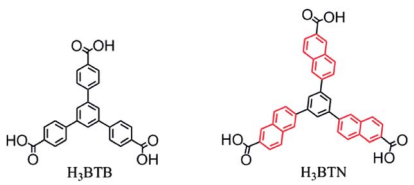

Scheme 1 Molecular structures of the ligands H_3BTB and H_3BTN.

Results and discussion

Synthesis and structure characterization

The solvothermal reaction of H_3BTN and $La(NO)_3·6H_2O$ in DMF (*N*,*N*′-dimethylformamide) containing benzoic acid leads to polyhedron-shaped brown crystals of [La(BTN)DMF]·solvent (PCP-1⊃guest). The structure was determined by single-crystal X-ray diffraction analysis, and was confirmed by the powder synchrotron X-ray diffraction pattern, measured at SPring-8 BL02B2 beamline (Fig. 1).[13] TGA shows that PCP-1 is thermally stable up to 500 °C under an N_2 atmosphere; this was further verified using varied temperature PXRD from 50 to 350 °C. After exchanging the guest solvents with methanol, we obtained the completely activated framework, degassed under a high vacuum at 120 °C for 20 hours, as indicated by the IR and TGA results of the evacuated PCP-1 (see the ESI†).

X-ray crystallography shows that PCP-1 crystallizes in the rare chiral space group of $P6_5$ with a = 34.2658(14) Å and c = 21.8681(14) Å. Three carboxylate groups of the BTN ligand have two coordination modes: bridging (μ_2-η^1:η^1), and chelating-bridging (μ_2-η^2:η^1), connecting to six La^{3+} ions. Each La^{3+} ion is coordinated by eight oxygen atoms from six carboxylate groups and one coordinated DMF molecule. The adjacent La^{3+} ions are bridged by three carboxylate groups, leading to edge-shared polyhedrons and an inorganic helical chain with a 21.85 Å screw pitch along the *c* axis. Each inorganic helical chain was linked to six neighboring chains by BTN ligands to form the 3D framework (Fig. 2). Compared with our previous La-BTB framework, the space between adjacent ligands has enlarged from ~3.8 Å to ~6.2 Å, which should provide a suitable space for CO_2 diffusion with low binding energy. Moreover, structural stability can also be expected because of the large coordination numbers of La^{3+}, the inorganic metal oxygen chain and the rigid ligand.

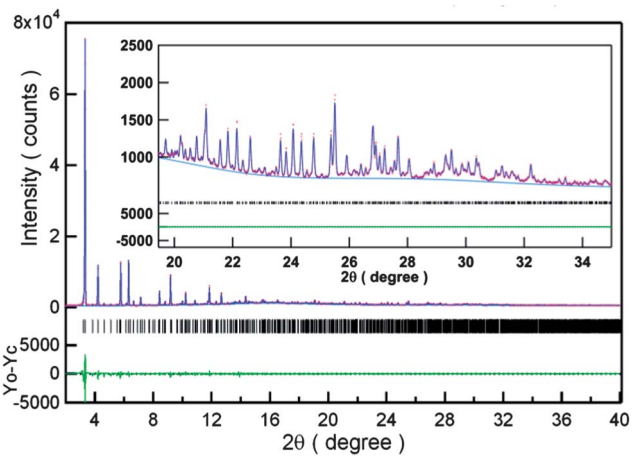

Fig. 1 The results of Le Bail analysis for the PXRD of PCP-1. The wavelength of an incident X-ray is 1.0 Å. Refined parameters and reliability factors are as follows: a = 34.5184(7) Å, c = 22.2682(10) Å, V = 22 978.2(12) $Å^3$. R_p = 0.0424 and R_{wp} = 0.0762.

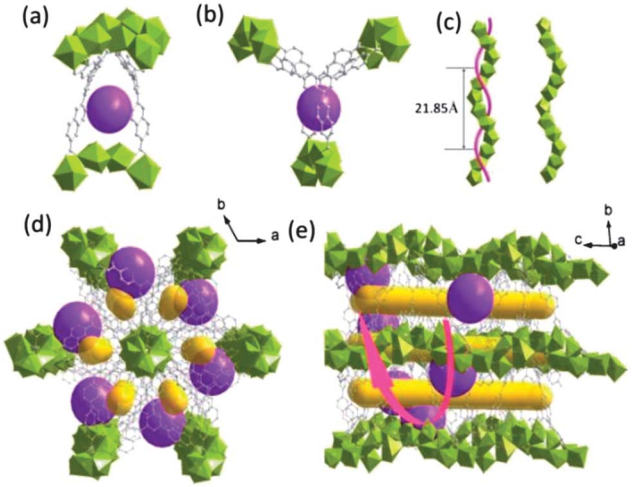

Fig. 2 The structure of PCP-1: accessible pore space between the two adjacent ligands from different directions (a) and (b); the helix chain in the framework (c); packing view of the 3D framework with two types of pore surface (d) and (e). 1D channel: yellow stick; irregular cage: pink ball.

Gas adsorption and IAST studies

To characterize the permanent porosity of PCP-1, a N_2 adsorption experiment was performed at 77 K. Since only micropores are present in PCP-1, a reversible type-I isotherm was observed. Furthermore, the distribution of the pore size, calculated from the N_2 adsorption profile, was around 0.55 nm, which agrees well with the pore-size parameter derived from the single crystal data.

To elucidate the gas uptake ability of PCP-1, single component gas-adsorption isotherms of CO_2, N_2, O_2 and CO were checked at 195 K and 273 K (Fig. 3a and c). The saturation adsorption amount of PCP-1 is 3.904 mmol g^{-1}, corresponding to about 2.8 molecules of CO_2 per BTN ligand. In addition, volumetric storage capacities, as one of the important standards of adsorbent materials in feasible applications, should also be considered.[14] Because the framework was constructed from the heavy La^{3+} metal chain and densely packed BTN ligands, PCP-1 has a high density (0.975 g cm^{-1}), but it also has a high uptake capacity of 167.1 g L^{-1} at 195 K. Importantly, even at 273 K and 1 bar, the uptake capacity of this PCP can reach 56.5 g L^{-1}, which is higher than that of some important porous materials, (La-BTB: 54.8 g L^{-1},[12] MOF-5: 39.9 g L^{-1},[15] and MOF-177: 50.7 g L^{-1} (at 298 K, 3.1 bar)[16]) and lower than that of some frameworks with functional amide groups (NTU-105: 227.0 g L^{-1},[17] Cu-TPBTM: 279.2 g L^{-1},[8e] and Cu-TDPAT, 344.8 g L^{-1} [18]). Meanwhile, the gas uptakes for N_2 and O_2 in these frameworks are also high, revealing the lower efficiency of selective capture of CO_2. In contrast, the uptakes of N_2, O_2 and CO in PCP-1 increase very slowly with the pressure. This may be because of the weaker interactions of these gases with the framework compared with that of CO_2. More importantly, the big gaps in uptake amounts around 10 kPa (CO_2: 2.93 mmol g^{-1}; N_2: 0.186 mmol g^{-1}; O_2: 0.199 mmol g^{-1}; CO: 0.302 mmol g^{-1}) indicate that PCP-1 is a good candidate for the selective capture of CO_2 from four-gas mixtures similar to flue gases.

The ideal adsorbed solution theory (IAST) of Myers and Prausnitz[19] is a well established method for describing gas mixture adsorption in many zeolites and PCP materials. We employed it to predict multi-component adsorption behaviors from the experimental single-component gas isotherms. As shown in Fig. 3b and d, PCP-1 exhibits high selective CO_2 capture in the following trend: $CO_2/N_2 > CO_2/O_2 > CO_2/CO$ at 195 K. At 273 K, the predicted selectivities (CO_2/N_2: ~93–38; CO_2/O_2: ~78–20 and CO_2/CO: ~68–18) are high enough (larger than 8) for the potential feasibility of the practical procedure.[11a]

Adsorption heat and NH_3-TPD studies

To understand such high separation ability better, the adsorption enthalpies of a series of PCPs were calculated using the Clausius–Clapeyron equation (Fig. 4). We note that the value of the isosteric heats of adsorption for PCP-1 is 28.5 kJ mol^{-1}, (26 kJ mol^{-1} by the virial method), which is lower than that of other materials with a high separation ability. This implies that the energy required for regeneration of the adsorbed CO_2 in fixed bed absorbers will be lower for PCP-1 than for MgMOF-74, NiMOF-74, Cu-TDPAT, CuBTC, or NaX zeolite. Usually, the Lewis acidity of the open metal site contributes greatly to the adsorption enthalpies. Here, the single crystal data indicate one coordinated DMF around the La^{3+} ions, but the IR and TGA results indicate the complete activation of evacuated PCP-1. Therefore, if the open metal site was generated in the activation process, the isosteric heats should be high. To find out why, temperature-programmed desorption (TPD) of NH_3 was used to examine whether or not the open metal site existed in PCP-1. As shown in the NH_3-TPD profiles (ESI†), there is only one signal for PCP-1 at temperatures ranging from 50 to 140 °C, which can be explained as the physical NH_3 adsorption on the channel surface of the materials (ESI†). In contrast, two signals can be found in MIL-101(Cr) which has a strong open metal site.[20] The first peak, around 200 to 300 °C, indicates the chemisorptions of NH_3 on the exposed chromium metal. The second peak (>300 °C) can be assigned to the partial decomposition of the structures, because the TGA results revealed that MIL-101(Cr) collapsed at high temperatures. Thus, here we can conclude that, after removing the coordinated DMF molecules, the coordination sphere of La^{3+} ions was slightly reorganized, and the exposed La^{3+} sites were recovered again by the other eight oxygen atoms.[21] Thus, only the large aromatics site of PCP-1 affords the binding energy to guest molecules.

Breakthrough simulations

To evaluate the gas separation ability of adsorbents under kinetic flowing gas conditions, breakthrough simulations were performed using a precise methodology established by Krishna and Long,[22] which are strongly pertinent to the pressure swing adsorption (PSA) process, an energetically efficient method for industrial scale capture. The breakthroughs of an equimolar four-component mixture including CO_2, N_2, O_2, and CO were

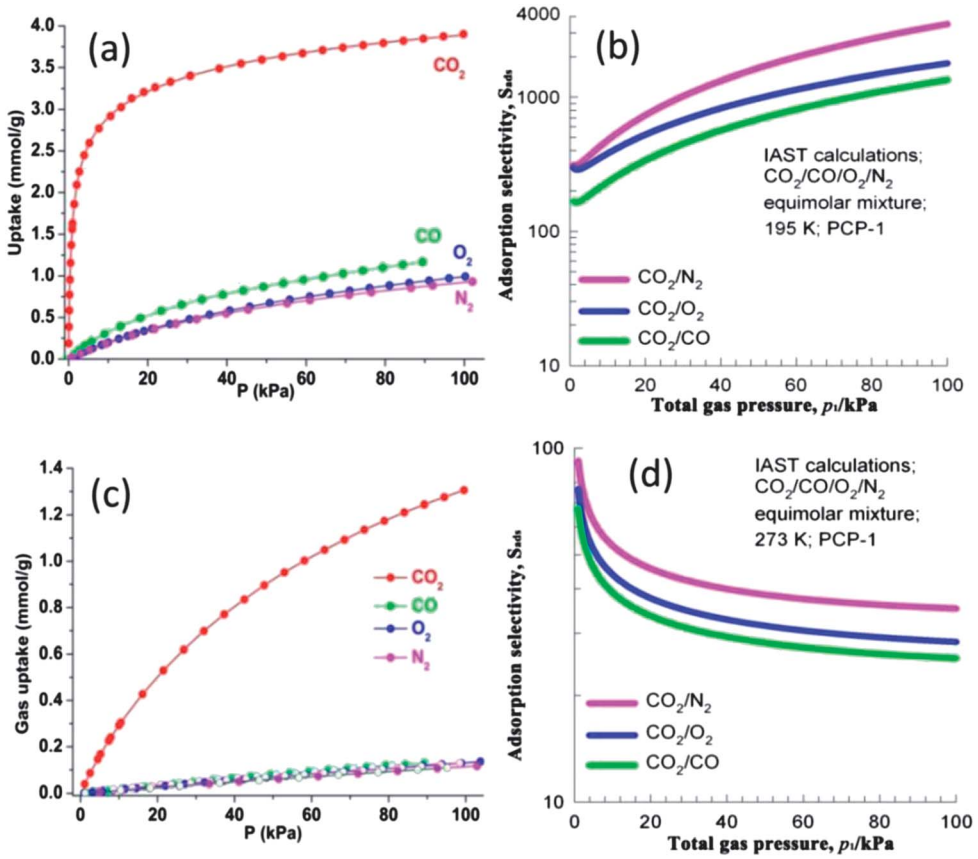

Fig. 3 Gas adsorption isotherms (circle points) and the dual-site Langmuir–Freundlich fit lines (lines) of CO_2, CO, O_2 and N_2 in PCP-1 at 195 K (a) and 273 K (100 kPa) (c). Calculations using the ideal adsorbed solution theory of Myers and Prausnitz for CO_2/CO, CO_2/O_2, and CO_2/N_2 selectivity for an equimolar quaternary CO_2–CO–O_2–N_2 gas mixture maintained at isothermal conditions at 195 K (b), and 273 K (d).

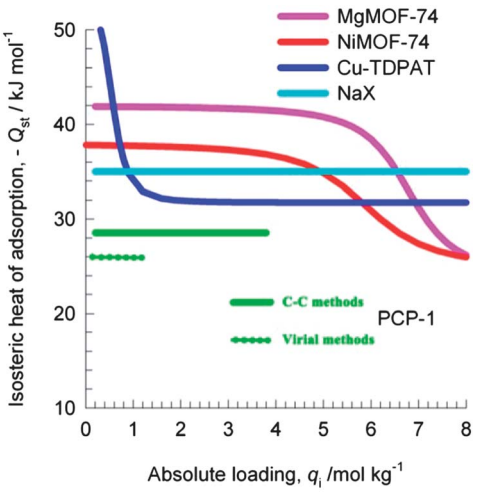

Fig. 4 Comparison of the isosteric heats of adsorption, Q_{st}, of CO_2 in PCP-1, MgMOF-74, NiMOF-74, Cu-TDPAT, CuBTC, and NaX zeolite.

explored at 195 K and 273 K. The partial pressures of these four gases were set as 25 kPa, and the relative concentrations of outflowing gas are shown in Fig. 5. The results indicate that at both temperatures, the sequence of breakthroughs is N_2, O_2, CO, and CO_2. The adsorption strengths of N_2, O_2 and CO are very similar, and their breakthroughs are also close together in time. CO_2, the component with the strongest adsorption strengths breaks through last.

Fig. S18† presents the breakthrough characteristics for CO_2–CO–O_2–N_2 (15/1/4/80) with a typical flue gas composition, operating at 195 K, and 273 K, respectively. Compared to the corresponding performance for equimolar mixtures, we note that the breakthrough of CO_2 occurs at significantly later times. This is because of the lower CO_2 content in the realistic flue gas mixtures, 15%. Longer breakthrough times imply a higher productivity in the fixed bed adsorber.[22]

In addition, the composition of flue gas changes frequently. It is therefore important to find out whether or not the gas composition can influence the breakthrough point. Fig. S15† presents breakthrough characteristics for binary 25/75 mixtures of CO_2–CO, CO_2–O_2, and CO_2–N_2 at 100 kPa, and 273 K. The breakthrough of CO_2 for all three binary mixtures occurs at approximately the same dimensionless time, $\tau = 70$, as for the quaternary mixture in Fig. 5, indicating that the separation capability of PCP-1 is not influenced by the gas composition. The significant time interval between the breakthroughs of CO, O_2, N_2 and CO_2 demonstrates that very good separation is possible in practice at ambient temperatures.

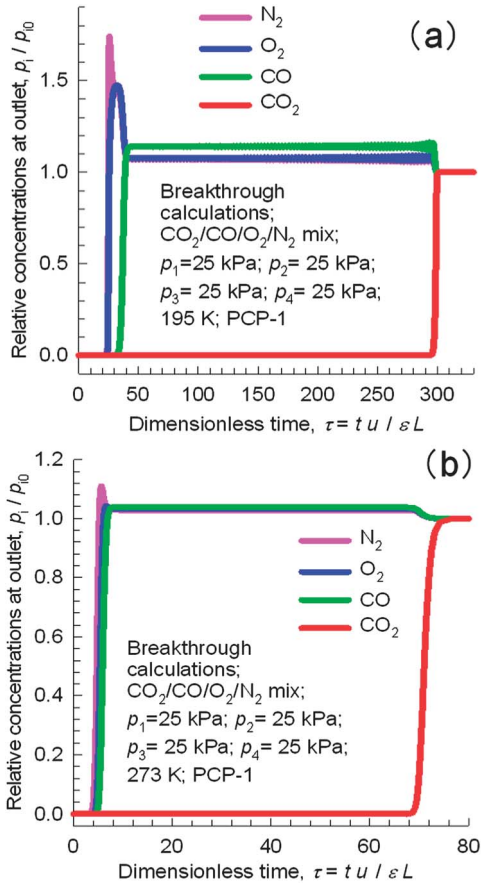

Fig. 5 Breakthrough characteristics of an adsorber packed with PCP-1 and maintained at isothermal conditions at 195 K (a) and 273 K (b). The inlet gas is a quaternary mixture CO_2–CO–O_2–N_2 at 100 kPa, with partial pressures for each component of 25 kPa.

Dynamic adsorption studies

Dynamic adsorption uptake is an important factor in the PSA process. Thus, we measured the temperature-dependent gravimetric adsorption cycling performance of PCP-1 with CO_2 using TGA (Fig. 6). After heating the evacuated samples at 150 °C for 40 min, the sample was cooled to 5 °C, and the temperature maintained for 20 min. Three cycles with mass change around 5 wt% were observed, and this value was almost equal to the pure CO_2 uptake. After the first cycle, the sample was exposed to air for 24 h, and a second cycle was performed. The gas uptake of PCP-1 does not change, indicating a good capture of CO_2 under kinetic flowing gas conditions. In addition, the desolvated sample of PCP-1 is a rigid framework during CO_2 adsorption, as verified by powder synchrotron X-ray diffraction (Fig. S22†).

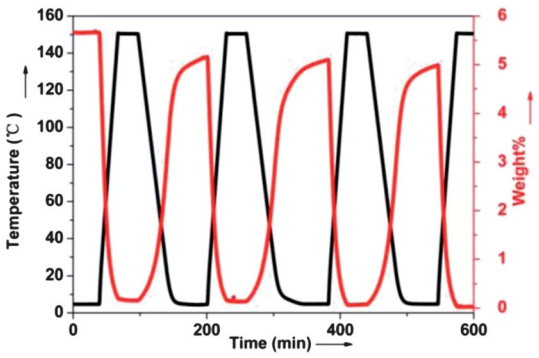

Fig. 6 Second cycle of the dynamic adsorption studies of PCP-1. Experimental mass changes are shown for pure CO_2 (red line). Flow rates are 50 mL min^{-1} and sample temperatures are plotted as the black line. The sample mass at 150 °C under each gas was normalized to 0%.

Thermal and chemical stability

With the good separation ability of CO_2 over CO, O_2 and N_2, we now explore the physical properties of PCP-1, especially its thermal and chemical stability, which can strongly affect the feasibility of practical applications.

X-ray thermodiffractometry of the as-synthesized PCP-1 was performed under a N_2 atmosphere from room temperature to 350 °C. As shown in Fig. 7, below 100 °C, some small peaks (2θ: from 20 to 30°) can be found in the PXRD results. Following the thermal treatment, these small peaks disappeared gradually, and the (0 3 1) and (1 1 3) peaks shifted very little to the low angle area. However, importantly, the position and the intensity of the (−1 1 1) peak did not change. Thus, it is reasonable to attribute such slight changes of the structure to the thermodiffractometry experiment and gas adsorption profiles, the removal of guest water and the following slight reorganization of the inherently flexible coordination sphere of La^{3+}. Similar phenomena have been reported in the complex of $\{[La_2(HL)_2(H_2O)_2(CO_3)](H_2O)_7\}_\infty$.[23] With the TGA data, we can conclude that the evacuated PCP-1 can maintain porosity to at least 350 °C.

Water and chemical stability are other important physical properties for the PCP sorbent.[24] Almost twenty thousand PCP/MOF structures have been reported to date; however, few of them can maintain their porosity after moisture, water and chemical treatment (La-BTB, MIL-100 and UiO-66),[12,25] as this is a key challenge for PCP/MOF chemistry. Hence, the evacuated PCP-1 was exposed to a moist 80% RH environment at various temperatures. The resulting PXRD patterns are the same as these of the original phase (Fig. 8). Encouraged by this good

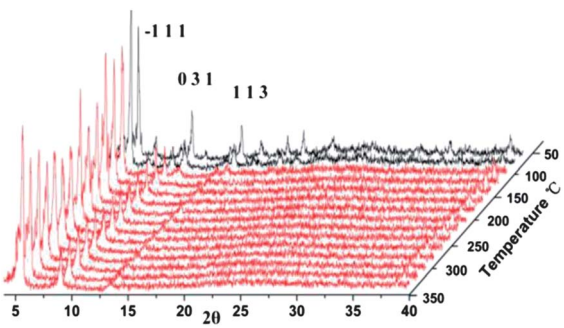

Fig. 7 X-ray thermodiffractograms of as-synthesized PCP-1 under N_2.

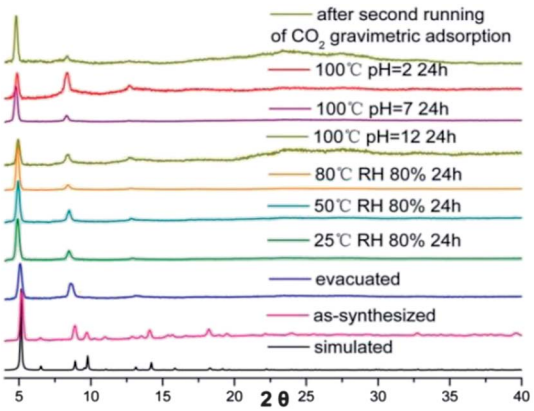

Fig. 8 PXRD patterns of PCP-1 after treatment.

result, the water and chemical stability of PCP-1 was examined by soaking the as-synthesized samples in harsh conditions: hot (100 °C) aqueous HCl (pH = 2), aqueous NaOH (pH = 12) and water solutions for one day. After cooling, the wet samples were checked by PXRD, which indicated the crystalline nature of the framework. To further demonstrate the integrity of the material, we performed CO_2 adsorption experiments at 195 K with PCP-1 which was treated in boiling water at different pH values for 24 h. The gas uptake of the treated PCP-1 (pH = 2 and 12) decreased a little, however, importantly, both the uptakes and shape of PCP-1 (pH = 7) are nearly identical with that of the fresh sample, exhibiting its high water and chemical stability (Fig. S21 and 22†). In addition, it is necessary to know the stability of degassed PCP-1 under moist environments at different temperatures, as it is difficult to avoid moisture in the industrial separation process, even though there is a much smaller amount. Compared with the isotherm of the fresh PCP-1, we found that the gas uptakes of the moisture treated PCP-1 decreased a little, however, importantly, after the second treatment, the gas uptakes are almost the same as their previous performance, despite the very harsh conditions (80 °C and RH% 80). Moreover, the gas uptakes of the treated PCP-1 are also almost the same at different temperatures, indicating high moisture stability of degassed PCP-1 (Fig. S23†). Taking the crystal structure into consideration, the high aqueous and chemical stability of PCP-1 could be assigned to the combination of the high coordination number of La^{3+}, the triangular ligand units and the coordination type. To our knowledge, because of the relatively weak metal–oxygen coordination, only a few carboxylate-bridged PCPs show structural stability in water for as long as a few hours at room temperature, while none have been shown to be stable in acid (pH = 2) or base (pH = 12) solutions at 100 °C for one day; however, this stability has been observed for zeolitic imidazole frameworks such as ZIF-8.[24c]

Conclusions

In summary, by moving the focus from the traditional open metal site and amide species for selective CO_2 capture, we have demonstrated a new robust porous coordination polymer, PCP-1, with larger aromatic rings. The experimental and simulated results all show that this framework satisfies the above four important prerequisites (suitable uptake, gas separation ability, water and chemical stability and appropriate binding energy) of potential porous materials for realizable separation applications. Given the unlimited scope of PCP chemistry, these four characteristics will become the targets in finding and constructing candidate porous materials for flue gas separation, especially in the PSA process.

Acknowledgements

We thank the financial support of the Japan Society for the Promotion of Science, ACT-C of the Japan Science and Technology Agency, WPI iCeMS program, "Quantum Ordering Research Project" launched in the RIKEN SPring-8 Center and the proposal of Japan Synchrotron Radiation Research Institute (no. 2013A1071). iCeMS is supported by the World Premier International Research Initiative (WPI) of MEXT, Japan.

Notes and references

1 J. Johnson, *Chem. Eng. News*, 2012, **90**, 8.
2 S. Chu, *Science*, 2009, **325**, 1599.
3 E. J. Granite and H. W. Pennline, *Ind. Eng. Chem. Res.*, 2002, **41**, 5470–5476.
4 (*a*) P. Nugent, Y. Belmabkhout, S. D. Burd, A. J. Cairns, R. Luebke, K. Forrest, T. Pham, S. Q. Ma, B. Space, L. Wojtas, M. Eddaoudi and M. J. Zaworotko, *Nature*, 2013, **495**, 80–84; (*b*) D. M. D'Alessandro, B. Smit and J. R. Long, *Angew. Chem., Int. Ed.*, 2010, **49**, 6058–6082; (*c*) J. R. Li, J. Sculley and H. C. Zhou, *Chem. Rev.*, 2012, **112**, 869–932; (*d*) S. Horike, Y. Inubushi, T. Hori, T. Fukushima and S. Kitagawa, *Chem. Sci.*, 2012, **3**, 116–120.
5 (*a*) R. Matsuda, R. Kitaura, S. Kitagawa, Y. Kubota, R. V. Belosludov, T. C. Kobayashi, H. Sakamoto, T. Chiba, M. Takata, Y. Kawazoe and Y. Mita, *Nature*, 2005, **436**, 238–241; (*b*) H. Furukawa, N. Ko, Y. B. Go, N. Aratani, S. B. Choi, E. Choi, A. O. Yazaydin, R. Q. Snurr, M. O'Keeffe, J. Kim and O. M. Yaghi, *Science*, 2010, **329**, 424–428; (*c*) G. Ferey, C. Mellot-Draznieks, C. Serre, F. Millange, J. Dutour, S. Surble and I. Margiolaki, *Science*, 2005, **309**, 2040–2042; (*d*) Y. S. Bae, C. Y. Lee, K. C. Kim, O. K. Farha, P. Nickias, J. T. Hupp, S. T. Nguyen and R. Q. Snurr, *Angew. Chem., Int. Ed.*, 2012, **51**, 1857–1860; (*e*) H. L. Jiang and Q. Xu, *Chem. Commun.*, 2011, **47**, 3351–3370; (*f*) L. J. Murray, M. Dinca and J. R. Long, *Chem. Soc. Rev.*, 2009, **38**, 1294–1314; (*g*) S. Kitagawa, R. Kitaura and S. Noro, *Angew. Chem., Int. Ed.*, 2004, **43**, 2334–2375.
6 S. C. Xiang, W. Zhou, Z. J. Zhang, M. A. Green, Y. Liu and B. L. Chen, *Angew. Chem., Int. Ed.*, 2010, **49**, 4615–4618.
7 (*a*) Y. K. Hwang, D. Y. Hong, J. S. Chang, S. H. Jhung, Y. K. Seo, J. Kim, A. Vimont, M. Daturi, C. Serre and G. Ferey, *Angew. Chem., Int. Ed.*, 2008, **47**, 4144–4148; (*b*) A. O. Yazaydin, A. I. Benin, S. A. Faheem, P. Jakubczak, J. J. Low, R. R. Willis and R. Q. Snurr, *Chem. Mater.*, 2009, **21**, 1425–1430.

8 (*a*) R. Vaidhyanathan, S. S. Iremonger, G. K. H. Shimizu, P. G. Boyd, S. Alavi and T. K. Woo, *Science*, 2010, **330**, 650–653; (*b*) J. An, S. J. Geib and N. L. Rosi, *J. Am. Chem. Soc.*, 2010, **132**, 38–39; (*c*) J. B. Lin, J. P. Zhang and X. M. Chen, *J. Am. Chem. Soc.*, 2010, **132**, 6654–6655; (*d*) J. G. Duan, Z. Yang, J. F. Bai, B. S. Zheng, Y. Z. Li and S. H. Li, *Chem. Commun.*, 2012, **48**, 3058–3060; (*e*) B. S. Zheng, J. F. Bai, J. G. Duan, L. Wojtas and M. J. Zaworotko, *J. Am. Chem. Soc.*, 2011, **133**, 748–751.

9 (*a*) D.-X. Xue, A. J. Cairns, Y. Belmabkhout, L. Wojtas, Y. Liu, M. H. Alkordi and M. Eddaoudi, *J. Am. Chem. Soc.*, 2013, **135**, 7660–7667; (*b*) T. Li, D. L. Chen, J. E. Sullivan, M. T. Kozlowski, J. K. Johnson and N. L. Rosi, *Chem. Sci.*, 2013, **4**, 1746–1755; (*c*) L. T. Du, Z. Y. Lu, K. Y. Zheng, J. Y. Wang, X. Zheng, Y. Pan, X. Z. You and J. F. Bai, *J. Am. Chem. Soc.*, 2013, **135**, 562–565; (*d*) T. M. McDonald, W. R. Lee, J. A. Mason, B. M. Wiers, C. S. Hong and J. R. Long, *J. Am. Chem. Soc.*, 2012, **134**, 7056–7065; (*e*) M. Wriedt, J. P. Sculley, A. A. Yakovenko, Y. G. Ma, G. J. Halder, P. B. Balbuena and H. C. Zhou, *Angew. Chem., Int. Ed.*, 2012, **51**, 9804–9808.

10 (*a*) S. S. Han, J. L. Mendoza-Cortes and W. A. Goddard, *Chem. Soc. Rev.*, 2009, **38**, 1460–1476; (*b*) S. Q. Ma, D. F. Sun, J. M. Simmons, C. D. Collier, D. Q. Yuan and H. C. Zhou, *J. Am. Chem. Soc.*, 2008, **130**, 1012–1016.

11 (*a*) Y. B. He, Z. J. Zhang, S. C. Xiang, F. R. Fronczek, R. Krishna and B. L. Chen, *Chem. Commun.*, 2012, **48**, 6493–6495; (*b*) O. K. Farha, Y. S. Bae, B. G. Hauser, A. M. Spokoyny, R. Q. Snurr, C. A. Mirkin and J. T. Hupp, *Chem. Commun.*, 2010, **46**, 1056–1058; (*c*) K. L. Mulfort and J. T. Hupp, *J. Am. Chem. Soc.*, 2007, **129**, 9604–9605.

12 J. Duan, M. Higuchi, S. Horike, M. L. Foo, K. P. Rao, Y. Inubushi, T. Fukushima and S. Kitagawa, *Adv. Funct. Mater.*, 2013, **23**, 3525–3530.

13 E. Nishibori, M. Takata, K. Kato, M. Sakata, Y. Kubota, S. Aoyagi, Y. Kuroiwa, M. Yamakawa and N. Ikeda, *Nucl. Instrum. Methods Phys. Res., Sect. A*, 2001, **467–468**, 1045–1048.

14 J. J. Purewal, D. Liu, J. Yang, A. Sudik, D. J. Siegel, S. Maurer and U. Muller, *Int. J. Hydrogen Energy*, 2012, **37**, 2723–2727.

15 K. S. Walton, A. R. Millward, D. Dubbeldam, H. Frost, J. J. Low, O. M. Yaghi and R. Q. Snurr, *J. Am. Chem. Soc.*, 2008, **130**, 406–407.

16 A. R. Millward and O. M. Yaghi, *J. Am. Chem. Soc.*, 2005, **127**, 17998–17999.

17 X. Wang, P. Li, Y. Chen, Q. Zhang, H. Zhang, X. Chan, R. Ganguly, Y. Li, J. Jiang and Y. Zhao, *Sci. Rep.*, 2013, **3**, 1149.

18 B. Li, Z. Zhang, Y. Li, K. Yao, Y. Zhu, Z. Deng, F. Yang, X. Zhou, G. Li, H. Wu, N. Nijem, Y. Chabal, Z. Lai, Y. Han, Z. Shi, S. Feng and J. Li, *Angew. Chem., Int. Ed.*, 2012, **51**, 1412–1415.

19 A. L. Myers and J. M. Prausnitz, *AIChE J.*, 1965, **11**, 121–122.

20 Y. Y. Pan, B. Z. Yuan, Y. W. Li and D. H. He, *Chem. Commun.*, 2010, **46**, 2280–2282.

21 T. Devic, V. Wagner, N. Guillou, A. Vimont, M. Haouas, M. Pascolini, C. Serre, J. Marrot, M. Daturi, F. Taulelle and G. Ferey, *Microporous Mesoporous Mater.*, 2011, **140**, 25–33.

22 R. Krishna and J. R. Long, *J. Phys. Chem. C*, 2011, **115**, 12941–12950.

23 J. Zhao, L. S. Long, R. B. Huang and L. S. Zheng, *Dalton Trans.*, 2008, 4714–4716.

24 (*a*) V. Colombo, S. Galli, H. J. Choi, G. D. Han, A. Maspero, G. Palmisano, N. Masciocchi and J. R. Long, *Chem. Sci.*, 2011, **2**, 1311–1319; (*b*) H. J. Choi, M. Dinca, A. Dailly and J. R. Long, *Energy Environ. Sci.*, 2010, **3**, 117–123; (*c*) K. S. Park, Z. Ni, A. P. Cote, J. Y. Choi, R. D. Huang, F. J. Uribe-Romo, H. K. Chae, M. O'Keeffe and O. M. Yaghi, *Proc. Natl. Acad. Sci. U. S. A.*, 2006, **103**, 10186–10191; (*d*) J. Taylor, R. Vaidhyanathan, S. Iremonger and G. Shimizu, *J. Am. Chem. Soc.*, 2012, **134**, 14338–14340; (*e*) H. Jiang, D. Feng, K. Wang, Z. Gu, Z. Wei, Y. Chen and H. Zhou, *J. Am. Chem. Soc.*, 2013, **135**, 13934–13938.

25 (*a*) K. A. Cychosz and A. J. Matzger, *Langmuir*, 2010, **26**, 17198–17202; (*b*) M. Kandiah, M. H. Nilsen, S. Usseglio, S. Jakobsen, U. Olsbye, M. Tilset, C. Larabi, E. A. Quadrelli, F. Bonino and K. P. Lillerud, *Chem. Mater.*, 2010, **22**, 6632–6640.

